Supporting Information

Visible-light-driven photoelectrochemical sensor based on conjugated microporous polymer-grafted graphene for *o*-aminophenol detection

Qiu jing Qin[1], Gang Xiang[1,2]*, Jiangfen Xu[4], Wenzhuo Li[3], Qinying Huang[1], Fengping Liu[1,2], Cuizhong Zhang[1,2], Zhengfa Zhang[1,2], Wei Huang[1,2], Jinyun Peng[1,2]*

[1]College of Chemical and Biological Engineering, Guangxi MinZu Normal University, Chongzuo 532200, China

[2]Photochemical Sensing and Regional Environmental Analysis Laboratory, Guangxi MinZu Normal University, Chongzuo 532200, China

[3]Institute for Food and Drug Control of ChongZuo, Chongzuo 532200, China

[4] Guangxi Institute for Drug Contyol, Nanning 530022, China

E-mail address: xgshmily@163.com (G. Xiang); pengjinyun@yeah.net(J.Y.Peng)

HPLC conditions were as follows:

HPLC analyses were carried out with a Shimadzu- C18 column (5 μm, 4.6 × 250mm) with Shimadzu HPLC system (Shimadzu, Kyoto, Japan) maintained at the temperature of 40°C. The mobile phase A was 0.1% formic acid in water, mobile phase B was 0.1% formic acid in acetonitrile. The elution was isocratic at a flow rate of 1.0 $mL \cdot min^{-1}$ with a mixture of mobile phases A and B in a ratio of 70:30. The PDA detector was set with an excitation wavelength of 280 nm for *o*-AP.

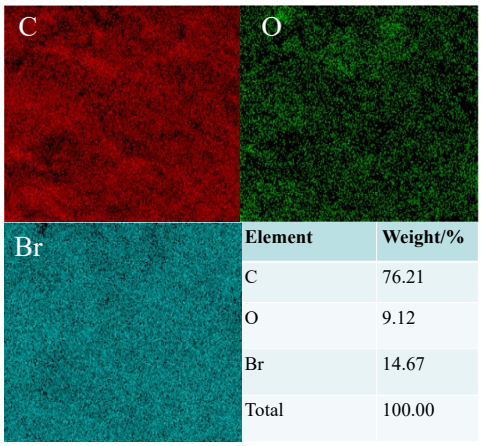

Element	Weight/%
C	76.21
O	9.12
Br	14.67
Total	100.00

Figure S1. EDS elemental mapping of rGBr

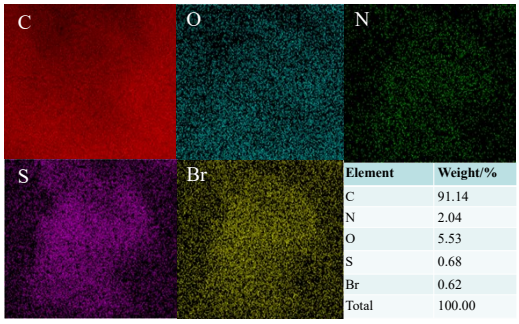

Element	Weight/%
C	91.14
N	2.04
O	5.53
S	0.68
Br	0.62
Total	100.00

Figure S2. EDS elemental mapping of CMP-rGO

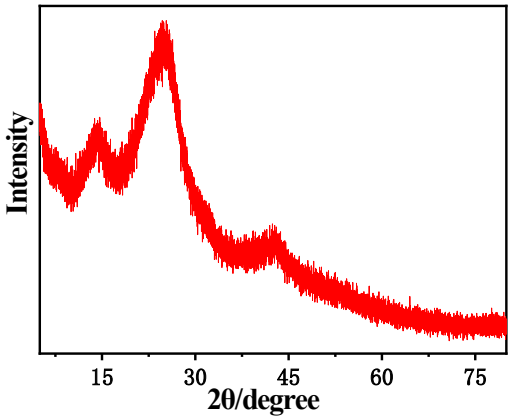

Figure S3.The XRD pattern of CMP-rGO

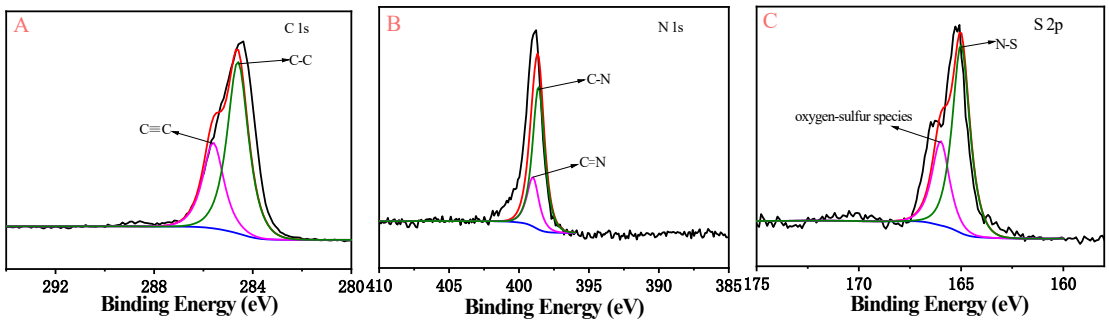

Figure S4. (A) C 1s spectrum, (B) N 1s spectrum, and (C) S 2p spectrum of XPS survey spectrum for CMP-rGO.

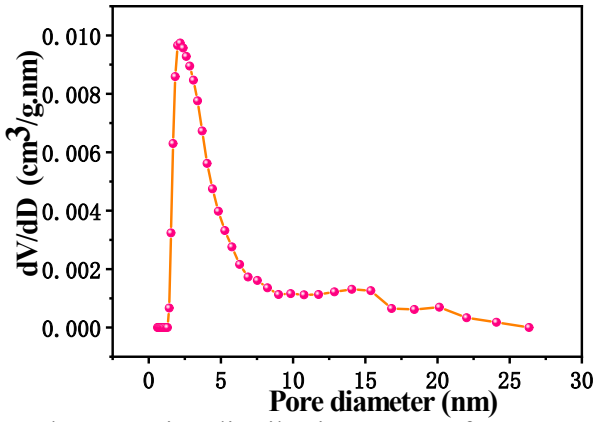

Figure S5. The pore size distribution curve of CMP-rGO

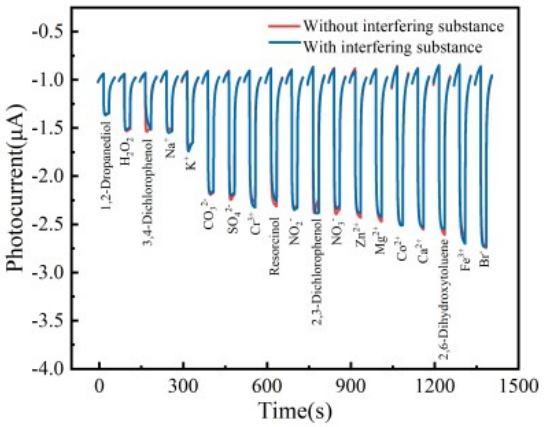

Figure S6. The intensity of the Photocurrent produced by the PEC sensor before and after 0.1 M PBS solution containing 11.25 μM of *o*-AP

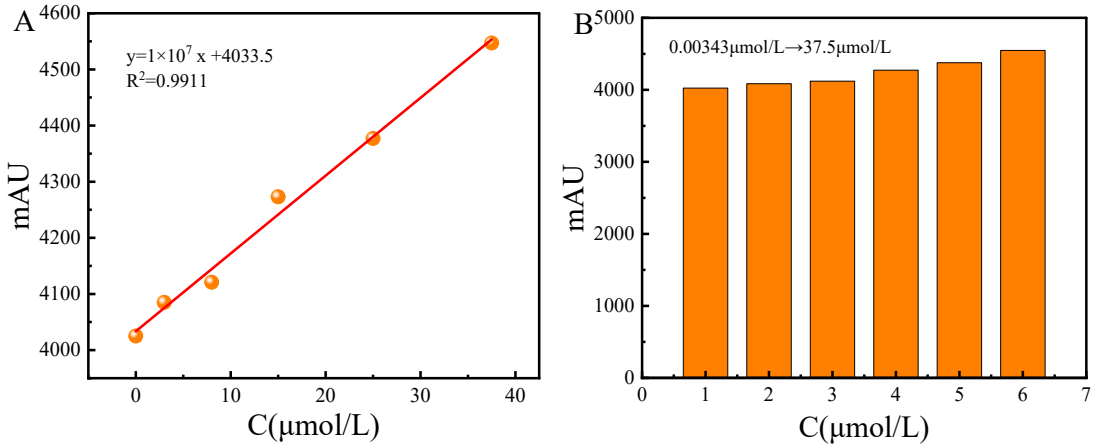

Figure S7. (A) Standard curve and (B) corresponding peak area histogram of OAP by HPLC detection.

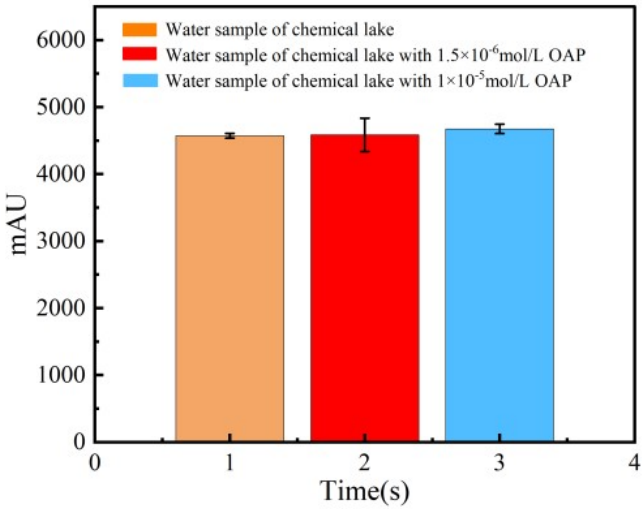

Figure S8. Histogram of peak area of OAP spiked recovery in real samples by HPLC (n=3)

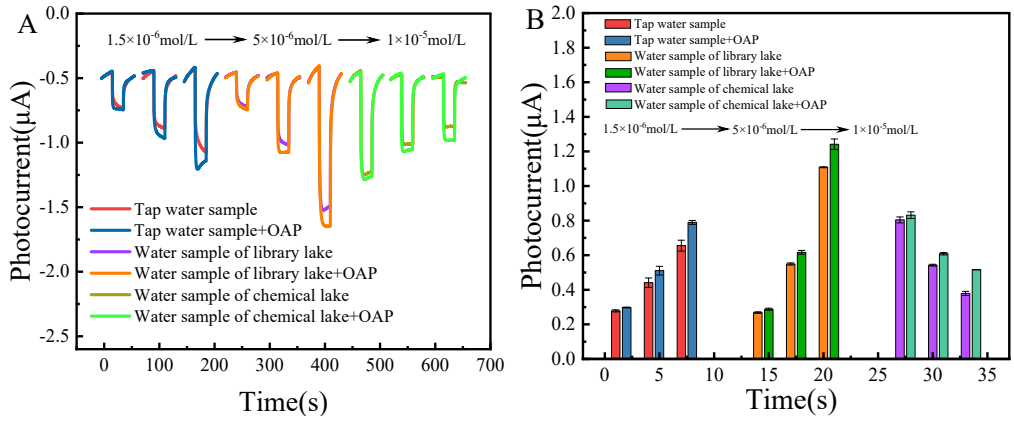

Figure S9. (A) Photocurrent and (B) bar graphs of actual sample spiking recoveries by PEC sensors (n=3)

Table.S1 The effect of interference for the detection of *o*-AP

Interfering substance	n	Er（%）	Interfering substance	n	Er（%）
Ascorbic acid	200	12.6	*m*-aminophenol	1	19.26
p-aminophenol	1	15.91	Catechol	1	112.2